

Real-time intra-store confocal Ca²⁺ imaging in isolated mouse cardiomyocytes

Miguel Fernandez-Tenorio, PhD, Ernst Niggli, MD,

Department of Physiology, University of Bern, 3012 Bern, Switzerland

Short title: Recording SR Ca²⁺

Address for correspondence:

Ernst Niggli
Department of Physiology
University of Bern
Bühlplatz 5
CH-3012 Bern
Switzerland

E-mail: niggli@pyl.unibe.ch

Phone: +41 31 631 8730

Fax: +41 31 631 4611

Number of words: 6260

Keywords: calcium signaling; excitation-contraction coupling; cardiac myocytes; confocal calcium imaging; sarcoplasmic reticulum

Abstract

To initiate the contraction of cardiomyocytes, Ca^{2+} is released from the SR to the cytosol via ryanodine receptors (RyRs), which are activated by the Ca^{2+} -induced Ca^{2+} release mechanism (CICR). The activity of RyRs is regulated by both, cytosolic and SR luminal Ca^{2+} . Deregulation of the CICR, by dysfunctional SR Ca^{2+} release or uptake, is frequently associated with cardiac pathologies (e.g. arrhythmias, CPVT, heart failure). Recently, the interest to directly measure changes of the free Ca^{2+} concentration within the SR ($[\text{Ca}^{2+}]_{\text{SR}}$) has led to the application of low affinity Ca^{2+} indicators (mag-fluo-4, Fluo-5N) to follow changes of $[\text{Ca}^{2+}]_{\text{SR}}$ in cardiomyocytes from some species. However, direct measurement of Ca^{2+} signals from the SR have not been possible in freshly isolated mouse cardiomyocytes. Here, we show a new protocol optimized to measure changes of $[\text{Ca}^{2+}]_{\text{SR}}$ in mouse cardiomyocytes using fluorescent Ca^{2+} indicators and confocal microscopy. The application of this protocol permits the design of experimental studies with direct evaluation of SR Ca^{2+} in real time in various mouse models of cardiac disease, including transgenic animals harboring mutants of RyRs or other Ca^{2+} signaling proteins. The technique, in combination with these models, will help to understand how these diseases and mutations affect Ca^{2+} signals within the SR and the Ca^{2+} sensitivity of the RyRs for cytosolic and SR luminal Ca^{2+} , thereby contributing to arrhythmias or weak heart beat.

1. Introduction

The intracellular Ca^{2+} concentration is a crucial second messenger for many processes such as muscle contraction, secretion, neuronal transmission, gene expression, cell migration, motility, fertilization, proliferation, etc. To optimize and target these signals to specific subcellular microdomains, most cell types have developed Ca^{2+} storing organelles, such as an endoplasmic or sarcoplasmic reticulum (ER or SR). Ca^{2+} uptake to and release from these stores allows for a highly organized spatio-temporal shaping of Ca^{2+} signals. In the heart and in cardiomyocytes, a transient increase of the cytosolic Ca^{2+} concentration is essential for excitation-contraction (EC) coupling. These changes of cytosolic Ca^{2+} can be measured and imaged using well established intensometric fluorescent Ca^{2+} indicators, which are frequently based on fluorescein (Fluo-3, -4 and related compounds) and rhodamine (Rhod-1, -2) [1,2] or with ratiometric Ca^{2+} dyes such as Fura-2 or Indo-1 [3,4].

In cardiomyocytes, the SR plays an important role as a Ca^{2+} store. During EC coupling Ca^{2+} is released into the cytosol via ryanodine receptor channels (RyRs). This signal is governed by the Ca^{2+} -induced Ca^{2+} release mechanism (CICR) which is serving as a Ca^{2+} signaling amplifier. Recently, it has become increasingly evident that disturbances of this Ca^{2+} release mechanism are involved in a wide range of pathologies (e.g. hypertrophy, cardiomyopathies, heart failure, channelopathies of the RyRs [5-11]). Abnormal and untimely Ca^{2+} release from the SR is known to be a key event in precipitating various forms of cardiac arrhythmias. Such diastolic Ca^{2+} release can, for example, be induced by SR Ca^{2+} overload, which is thought to make the RyRs more sensitive for Ca^{2+} . RyRs have been proposed to sense the Ca^{2+} concentration inside the SR via an allosteric signal involving calsequestrin, triadin and junctin [12]. Recently, it has been shown that the RyRs can also sense the Ca^{2+} concentration inside the SR directly [13,14]. Alterations of the free SR Ca^{2+} concentration ($[\text{Ca}^{2+}]_{\text{SR}}$) can be explained by a variety of dysfunctions of elements that participate in the SR Ca^{2+} uptake/release balance (e.g. SERCA and RyR, for review see [6]). In addition, the RyRs themselves can become abnormally Ca^{2+} sensitive, either as a result of posttranslational protein modifications (e.g. phosphorylation, oxidation), or because of arrhythmogenic RyR mutations, which are frequently underlying catecholaminergic polymorphic ventricular tachycardias (CPVTs).

Because of its emergent pathological importance, direct and time resolved measurements of free $[Ca^{2+}]_{SR}$ have become much more desirable over the last decade. This is particularly true because of the recent availability of various animal disease models, such as transgenic mice harboring channelopathies initially identified in human patients. Several methods have been described to experimentally estimate the amount of Ca^{2+} stored in the SR, but only indirectly. Puffs of the RyR agonist caffeine applied to isolated cardiomyocytes allow to estimate the amount of SR Ca^{2+} , either by recording the amplitude of the triggered cytosolic Ca^{2+} transient or by integrating the resulting inward current through the Na^+/Ca^{2+} exchanger (as a consequence of Ca^{2+} extrusion, for example see [15-18]). These methods have considerable limitations, as they are static measurements and only can estimate SR Ca^{2+} content at one or a few defined moments during the experiment. Moreover, these measurements do not allow to extract any spatial information about free $[Ca^{2+}]_{SR}$ and can be rendered inaccurate by Ca^{2+} release events occurring just before the caffeine application. All these drawbacks have intensified the need to measure $[Ca^{2+}]_{SR}$ directly. Concurrently with the emergence of genetic probes, methods based on chemical low affinity Ca^{2+} indicators have been developed (mag-fluo-4, Fluo-5N) to quantify changes of $[Ca^{2+}]_{SR}$. Mag-fluo-4 has been applied to detect changes of $[Ca^{2+}]_{SR}$ of uterine smooth muscle [19] and in intact mouse heart [20,21]. Fluo-5N has been used to measure SR Ca^{2+} , initially in frog skeletal muscle [22] and later in single cardiomyocytes isolated from rabbit [23,24] and dog hearts [9]. The intra SR Ca^{2+} signals recorded from such preparations exhibited good signal-to-noise ratios, adequate spatial resolution and very fast kinetics. But targeting of the indicators to the SR by the AM-ester loading technique has remained a challenge.

Unfortunately, direct measurement of SR Ca^{2+} signals have not yet been accomplished in freshly isolated mouse cardiomyocytes. This is particularly disappointing given the wide availability of mouse models for cardiac diseases. In this paper, we introduce a new and optimized protocol to measure SR Ca^{2+} signals in freshly isolated mouse cardiomyocytes. Dialysis via patch-clamp electrode, irreversible and reversible permeabilization with saponin and streptolysin-O, respectively, were used to remove contaminations of Fluo-5N entrapped in the cytosol. We applied electrophysiological and confocal imaging techniques to simultaneously acquire cytosolic (high-affinity Ca^{2+} indicator Rhod-2) and SR (Fluo-5N) Ca^{2+} signals in patch-clamped cardiomyocytes

while recording Ca^{2+} currents which triggered SR Ca^{2+} release. In addition, we were able to record potentially arrhythmogenic cytosolic and intra-SR Ca^{2+} waves in permeabilized mouse cardiomyocytes.

A protocol to measure changes of free $[\text{Ca}^{2+}]_{\text{SR}}$ in mouse cardiomyocytes will find applications in multiple experimental studies and in a wide range of mouse models of cardiac disease. Besides established murine heart failure models, this can also be transgenic mice harboring, for example, the aforementioned RyR channelopathies or mutations in other Ca^{2+} signaling proteins recapitulating identified human pathologies. Studies using this technique will substantially contribute to our understanding of how these diseases and mutations affect SR Ca^{2+} in ways which can trigger dangerous arrhythmias or cardiac death. Since RyRs are regulated by both, cytosolic and luminal Ca^{2+} and because mutations in RYRs could modify their sensitivity to Ca^{2+} , this protocol will be particularly useful to study how changes in free $[\text{Ca}^{2+}]_{\text{SR}}$ regulate the RyR activity.

2. Methods

Important features of the technique will be described in the “Procedures and Results” chapter below. An expanded and more detailed description of the protocol is available in the online-only supplement.

2.1 Cell isolation

The animal care and breeding, and all experiments were carried out following the animal handling procedures conforming with the Guide for the Care and Use of Laboratory Animals published by the US National Institutes of Health and National Research Council of the National Academy of Sciences (NIH Publication No. 85-23, revised 2011) and with the permission of the State Veterinary Administration and according to Swiss Federal Animal protection law (permit BE126/12). Animals were euthanized by cervical dislocation, heart was rapidly removed and cardiomyocytes were isolated by enzymatic dissociation.

2.2 Measurements of SR Ca^{2+} concentration

To measure Ca^{2+} changes in cytosol and SR, the Ca^{2+} dyes, Fluo-5N and Rhod-2 (low- and high- Ca^{2+} indicator, respectively) were used. Ca^{2+} images (x,y) and line-scan recordings (x,t) were acquired with a FluoView 1000 (Olympus) laser-scanning confocal microscope. Ca^{2+} indicators were excited at 488 nm with a solid-state laser (Sapphire 488-10). Fluo-5N fluorescence (i.e. the intra-SR signal) was detected between 515 and 560 nm, and >585 nm for Rhod-2 (i.e. the cytosolic signal). Images were processed and analyzed using the software ImageJ (NIH).

2.3 Patch-clamp technique

The patch clamp technique was used in the whole cell configuration and in voltage-clamp mode to wash out the small amount of residual Fluo-5N entrapped in the cytosol (instead of the SR), to dialyze Rhod-2 salt (50 $\mu\text{mol/L}$) into the cytosol and to control the plasma membrane voltage.

2.4 Permeabilization with saponin

To completely wash out the residual Fluo-5N content of the cytosol the cells were irreversibly permeabilized using a protocol based on the disruption of the plasma membrane with saponin.

2.5 Reversible permeabilization with Streptolysin O

This technique was adapted from a previously published protocol [26], as an alternative possibility to eliminate residual Fluo-5N from the cytosol and to introduce Rhod-2 salt.

3. Procedures and Results

3.1 Optimizing cardiomyocyte isolation and Fluo-5N loading

To optimize the loading of the SR with the indicator Fluo-5N, the quality and yield of the enzymatic cardiomyocyte isolation turned out to be of decisive importance. For details of the methods, solutions and protocols see the online supplement including Fig. S1. We first analyzed the viability of the ventricular myocytes after the enzymatic cell isolation and later following the stepwise increments of the extracellular Ca^{2+} concentration ($[\text{Ca}^{2+}]_o$). Usually, the proportion of healthy cells (with a rod-shaped morphology) was 60 ± 5.5 % immediately after the isolation and 53 ± 6.9 % after increasing $[\text{Ca}^{2+}]_o$. The fraction of healthy cells stayed at 38.4 ± 6.2 %, even within 4 hours after the isolation. This percentage improved to 49 ± 5.4 % when the solution was supplemented with BSA (0.5%) after the last increment of $[\text{Ca}^{2+}]_o$. The quantification of the fraction of viable cells was expected to be important, because damaged cells will release intracellular material, including cellular esterases and proteases, to the medium. These enzymes may damage the viable cells and degrade the AM-ester form of Fluo-5N during the loading process. Thereby, these enzymes can interfere with cardiomyocyte dye uptake, particularly during the relatively long loading procedure required for SR loading (see Fig. S1B). Therefore, we compared the quality of Fluo-5N loading in several isolations of cardiomyocytes with different percentages of healthy cells. To quantify the efficiency of the indicator loading and targeting into the SR the characteristic intra-organellar distribution of the dye inside the SR was analyzed. As Fig. 1 shows, Fluo-5N was distributed in parallel and transversal bright lines, with a spacing of approximately $1.8 \mu\text{m}$, which is corresponding to the common sarcomeric architecture of the junctional SR in resting myocytes. This is seen as periodic intensity fluctuations in a profile of fluorescence which was taken along the longitudinal cell axis (yellow line, Fig. 1B), whereas the transversal profiles along the junctional and free SR did not show such a periodicity (Fig. 1D). Since the lumen of the nuclear envelope is contiguous with the SR, this compartment was also intensely labeled with Fluo-5N. We determined that in order to obtain a high efficiency of Fluo-5N loading, the ratio of viable to damaged cells immediately after isolation needs to be higher than 3:2 and the medium has to be supplemented with 0.5% of BSA. The addition of 100

$\mu\text{mol/L}$ phenylmethylsulfonyl fluoride (PMSF), which reversibly inhibits the activity of esterases and proteases (released from damaged cells) during Fluo-5N AM incubation, leads to a further substantial improvement of the SR Fluo-5N loading (Fig. 1E). Taken together these results indicate that the efficiency of SR loading with Fluo-5N can be impaired by de-esterification of the AM ester form of the dye in the loading buffer. Therefore, minimizing cell damage and the subsequent esterase release to the medium, as well as the inhibition of any residual esterase activity, are decisive to obtain a sufficient quality of Fluo-5N loading into the SR. In addition, partial inhibition of intracellular (i.e. cytosolic) esterases by the reversible inhibitors may also contribute to this improvement, by allowing a less restricted diffusion of the AM esters across the cytosol into the SR.

3.2 Residual cytosolic Fluo-5N contamination and methods to remove it

One difficulty of the SR loading with Fluo-5N AM is that the organelle targeting is far from perfect. For example, other organelles, such as mitochondria, may take up the indicator, particularly if the loading time is very long. Despite precisely timed loading protocols, there will be a small amount of de-esterified Fluo-5N in the cytosol. Even though the concentration of Fluo-5N in the cytosol was quite small, in comparison to the amount of dye in the SR, and the affinity for Ca^{2+} is very low ($\sim 90 \mu\text{mol/L}$ in vitro and $\sim 400 \mu\text{mol/L}$ in vivo [23,25]), contaminating cytosolic Ca^{2+} signals could still be detected. This was noticeable, for example, in experiments involving the application of caffeine (10 mmol/L), a RyR agonist which generates a very large and synchronized Ca^{2+} release from the SR. In such experiments, an increase of the Fluo-5N fluorescence could be clearly resolved, before the SR emptying became apparent (see phase 2 in Fig. 2B and 2C). To solve the problem of cytosolic contamination, we tried a range of different approaches to remove Fluo-5N from the cytosolic compartment: 1) The patch clamp technique in the whole-cell configuration to dialyze the residual Fluo-5N out of the cell. 2) Irreversible permeabilization of the cell membrane with saponin. 3) Reversible permeabilization with streptolysin O (SLO), a procedure which allowed partial recovery of the plasma membrane properties.

3.3 Cell dialysis with patch clamp pipette

In its whole-cell configuration, the patch clamp technique not only allows us to control the membrane voltage, but also permits solution exchange between the cytosol and the patch pipette, typically used to load the cells with chemical compounds, such as fluorescent indicators. We have used this feature to dialyze out and minimize residual Fluo-5N in the cytosol (Fig. 3A). To examine whether the extent of dye removal via the patch pipette is appropriate, we dialyzed the cells during more than 10 min. After this interval, we stimulated the myocytes electrically and simultaneously recorded the cytosolic and intra-SR Ca^{2+} signals. Voltage-clamp depolarizations from -80 mV to 0 mV induced transient elevations of cytosolic Ca^{2+} (Rhod-2 channel, in red), mediated by Ca^{2+} influx through L-type Ca^{2+} channels and SR Ca^{2+} release via RyRs (Fig. 3B). As a consequence of the SR Ca^{2+} release the Ca^{2+} concentration inside the SR decreased, indicated by the decline in Fluo-5N fluorescence. After successfully dialyzing out the cytosolic Fluo-5N via patch clamp pipette, we no longer observed a transient increase of Fluo-5N fluorescence resulting from contamination (compare with the signal elicited by caffeine in Fig. 2C). These results confirmed that dialysis via a patch-clamp pipette is suitable to remove the Fluo-5N dye contamination from the cytosol. However, to obtain a complete Fluo-5N wash out the cells needed to be dialyzed via the patch-pipette during at least 10 min. This requirement may limit the amount of experimental time available for each cell. The contractions and related motion artefacts were blocked using 10 mmol/L of 2,3-butanedione 2-monoxime (BDM).

3.4 Permeabilization with saponin

For Ca^{2+} signals not requiring electrical activity and a functioning cell membrane (for example Ca^{2+} waves and Ca^{2+} sparks) we used a technique based on the permeabilization of the sarcolemma to allow removal of residual cytosolic Fluo-5N by simple diffusion. For the permeabilization of the cell membrane, we briefly exposed the myocytes to saponin (around 30 seconds), which binds to cholesterol molecules in the sarcolemma generating micelles and pores in the membrane (Fig. 4A). To determine the efficiency of this method to remove the residual cytosolic Fluo-5N we analyzed the fluorescence changes evoked by Ca^{2+} transients induced by caffeine. In Fig. 4B, an increase of the

Rhod-2 fluorescence can be observed following caffeine application, due to Ca^{2+} release into the cytosol via RyRs. Simultaneously, the Fluo-5N fluorescence intensity decreased. Please note the absence of an initial cytosolic Fluo-5N spike at the beginning of the exposure to caffeine (compare with Fig. 2C). Therefore, we can conclude that the permeabilization protocol is an efficient way to remove the contaminating Fluo-5N from the cytosol. Please also note that, in contrast to analogous Ca^{2+} signals in an intact cell, the decline of the cytosolic Ca^{2+} transient is not the consequence of re-uptake into the SR and extrusion via the Na^+ - Ca^{2+} exchange, but rather is largely governed by diffusion of Ca^{2+} into the large volume of bath solution surrounding the permeabilized myocyte. We next assessed whether this protocol offers sufficient sensitivity to study smaller SR- Ca^{2+} changes, such as spontaneous Ca^{2+} waves or even local Ca^{2+} depletions, the intra-SR equivalent of a cytosolic local Ca^{2+} signal [24,26]. The cytosolic Ca^{2+} wave detected by Rhod-2 during a Ca^{2+} wave was accompanied by a corresponding drop of the Fluo-5N fluorescence (Fig. 4C, upper panel). In order to extract the time course of both, the cytosolic and intra-SR Ca^{2+} wave, the line-scan images needed to be de-skewed using a custom-written ImageJ macro. This synchronizes and aligns the wave-fronts (for details see the online supplement). After this image processing step the true time-course of the Ca^{2+} waves can be extracted from the confocal line-scans (compare black and grey traces in Fig. 4C, lower panel). As is shown in Fig. 4D, Fluo-5N detection is also sufficiently sensitive to reveal the SR Ca^{2+} changes evoked by the depletion during a local Ca^{2+} signal.

3.5 Reversible permeabilization with streptolysin O

As mentioned in the previous section, permeabilization with saponin is a suitable approach to remove Fluo-5N from the cytosol, but it does not allow to study SR Ca^{2+} release signals which are modulated by receptors located in the sarcolemma (e.g. the β -adrenergic receptor signaling pathway). Therefore, a reversible permeabilization approach using streptolysin O (SLO) was attempted (protocol see Fig. S1C). SLO is a hemolytic toxin which forms pores in the sarcolemma in a transient and reversible fashion [27]. The reversibility of this technique is based on the property of SLO to bind to sarcolemmal cholesterol molecules and to form pores only under reducing conditions. After re-establishing a normal redox environment, the pores close and disappear, thereby making the

permeabilization reversible (Fig. 5A). To test whether this technique is suitable to allow the exchange of small molecules between the cytosol and extracellular medium, we evaluated the uptake and retention of Rhod-2 pentapotassium salt (the membrane impermeable form of this Ca^{2+} indicator) into the cells. Cells exposed to extracellular Rhod-2 during the reversible permeabilization showed cytosolic Ca^{2+} signals (see Ca^{2+} waves in Fig. 5B), confirming that the Ca^{2+} indicator was incorporated into the cells. To assess membrane integrity further, myocytes were incubated with a high Ca^{2+} concentration in the external solution (6 mmol/L, Fig. 5B). Many cells resisted such elevated external Ca^{2+} concentrations and some showed clearly observable Ca^{2+} waves, which resulted from SR Ca^{2+} overload, as expected (Fig. 5B). To assess whether the β -adrenergic signaling pathway remained intact despite the reversible permeabilization, 1 $\mu\text{mol/L}$ isoproterenol (ISO) was added to cells exhibiting Ca^{2+} waves (Fig. 5B and C). The propagation velocity and the Ca^{2+} wave amplitude were larger after 3 and 6 minutes in ISO, respectively. In addition, the τ of wave decay became shorter. Together, these results confirm a stimulation of the SR Ca^{2+} pump (SERCA) as a result of β -adrenergic receptor stimulation. Ca^{2+} waves recorded from the SR of Ca^{2+} overloaded myocytes exhibited no initial overshoot of the Fluo-5N signal, suggesting successful removal of any residual cytosolic Fluo-5N during the reversible permeabilization (Fig. 5D).

4. Method validation and discussion

To document and validate the broad applicability of this new protocol, several experiments were carried out. First, we tested whether the technique can detect changes in the level of relative $[Ca^{2+}]_{SR}$ required to initiate spontaneous Ca^{2+} waves. Such changes of Ca^{2+} wave threshold are thought to play a central role in the precipitation of cardiac arrhythmias. While an abnormally high RyR Ca^{2+} sensitivity has been widely recognized to be an arrhythmogenic substrate, it has only recently been reported that, surprisingly, a reduced sensitivity due to a loss-of function RyR mutation can likewise precipitate arrhythmias [28]. To experimentally and acutely simulate an abnormally elevated RyR Ca^{2+} sensitivity, a low concentration of caffeine (200 μ mol/L) was added to the internal solution [29]. This provoked an increase in the frequency of Ca^{2+} waves (Fig. 6A), evidently because the threshold for Ca^{2+} wave initiation was lowered and therefore was reached earlier. Each Ca^{2+} wave depleted the SR of some Ca^{2+} and the gradually declining wave threshold prevented refilling of the SR back to the control level. Thus, each recurring Ca^{2+} wave caused a net loss of Ca^{2+} from the SR and its content decreased in a stepwise fashion. In parallel, the lowered SR content led to a reduction of the Ca^{2+} wave amplitude. Taken together, we observed that at high RyR Ca^{2+} sensitivity the intensity of the SR fluorescence at which the Ca^{2+} waves were initiated was lower than in control conditions, consistent with a lower trigger threshold for SR Ca^{2+} release. This is in accordance with a previous publication [29], where Ca^{2+} waves have been measured and SR Ca^{2+} has been numerically determined from the involved Ca^{2+} fluxes. These results confirm that this new protocol to measure SR Ca^{2+} can detect small changes in the Ca^{2+} threshold to generate Ca^{2+} waves.

Previously, it has been shown that absolute Ca^{2+} release amplitudes can be compared between different cells by using a normalization procedure based on the the level of Fluo-5N fluorescence during the application of high concentrations of caffeine (10 mmol/L) as a reference (F_{Caff}) [23]. In caffeine, the RyRs remain open and the $[Ca^{2+}]_{SR}$ ultimately declines to the $[Ca^{2+}]_{cyt}$ (~100 nmol/L). Fig. 6B shows that such a high concentration of caffeine induced a decrease of the SR fluorescence signal in our preparation, similar to previous studies [9,23]. Therefore, the minimal fluorescence value during caffeine application can be used to normalize the SR signal for variable Fluo-5N loading, since the absolute level reached in caffeine mainly depends on the amount of Fluo-5N entrapped in the SR.

When converting the Fluo-5N signals into absolute intra-SR Ca^{2+} concentrations, a small quench of the Fluo-5N fluorescence by caffeine would need to be considered (see supplement).

Taken together, these findings show that with the developed protocol adequate Fluo-5N targeting to the SR and confocal imaging of the intra-SR Ca^{2+} concentration with good spatial and temporal resolution is feasible in mouse cardiomyocytes. Besides optimal conditions and timing of the loading period, preventing (and inhibiting) the activity of esterases in the incubation medium (and in the cytosol of the cardiomyocytes) appeared to be decisive approaches to enable the use of this powerful technique also in mouse cardiomyocytes.

Limitations of the technique:

The technique described here allows to record changes of the free SR Ca^{2+} concentration with reasonable temporal and spatial resolution. Obviously, to estimate total SR Ca^{2+} content other approaches are required (e.g. caffeine puffs). But free SR Ca^{2+} recordings are quite challenging and limited by several constraints. As described above in detail, cytosolic Fluo-5N contamination can be an issue, but there are techniques to solve this problem. The reversible permeabilization has the additional limitation that field stimulation results in very small SR Ca^{2+} depletions (when compared to those observed during Ca^{2+} waves, data not shown). The reason for this is unknown to us, but it is a peculiarity which should be considered when designing field-stimulation experiments using this approach to remove residual cytosolic Fluo-5N. Another limitation is related to the small volume of the SR (3-6 % of the total cell volume). This leads to the availability of only a small amount of Fluo-5N indicator. In combination with the relatively poor signal-to-noise ratio, this accentuates difficulties arising from dye bleaching. To improve the recording system for this challenge, it is of utmost importance that the fluorescence detection is optimized, for example by using emission filters with the maximal allowable bandwidth or by using detectors with a high sensitivity. If diffraction limited spatial resolution is not a concern, the pin-hole of the confocal laser scanning microscope can be opened to some extent, allowing for more photons to be detected. Nevertheless, some photobleaching is inevitable in such recordings. Since bleaching usually follows a monoexponential time-course, a correction for photobleaching can be employed during data analysis. Motion artefacts are another

potential problem of the recordings from the SR, particularly during full cellular Ca^{2+} transients. BDM or blebbistatin can be used to minimize motion during such experiments (see Fig. 3B), but side-effects of these unspecific compounds need to be considered in such experiments.

As far as targeting to an organelle is concerned, genetic Ca^{2+} indicators would be more specific. For ER and SR measurements, fusion proteins based on variants of GFP, calmodulin or troponin as low affinity Ca^{2+} sensors have been developed (ER-targeted FP: cameleons er-3 and er-4 [30], D1ER [31-33], for review see [34]). In cultured neonatal cardiomyocytes SR-targeted yellow cameleons (YC3er, YC4er) have been expressed and used to record Ca^{2+} ratiometrically (using FRET) from the SR [35]. Unfortunately, expression of genetic indicators in primary cardiomyocyte cultures has some critical limitations. These cells are quite challenging to transfect, often requiring viral constructs [36]. In addition, fully differentiated adult cardiomyocytes in culture undergo very rapid dedifferentiation with disappearance of the t-tubules and therefore collapse of EC-coupling within 24 to 48 hours [37]. Since the viral transfection approaches mentioned above require substantial time for sufficient protein expression, the usefulness of genetic Ca^{2+} indicator techniques in freshly isolated cardiomyocytes is very limited and the chemical probes are therefore far superior for acute application. For the future, the generation of animal models expressing an SR targeted Ca^{2+} indicator might be a promising possibility (see [38] for a mouse model conditionally expressing a cytosolic Ca^{2+} indicator).

In conclusion, the adapted protocol to load Fluo-5N AM into the SR of freshly isolated mouse cardiomyocytes allows to acquire recordings of SR- Ca^{2+} changes during up to several minutes. To have this ability at hand will be a very powerful tool to define alterations of intra-SR Ca^{2+} signaling in various mouse models of cardiac disease, including those resulting from mutations of Ca^{2+} signaling proteins (i.e. RyR, SERCA, CaM, PLB or calsequestrin mutants). Changes of intra-SR Ca^{2+} handling may be clinically relevant, as they are linked to cardiac arrhythmias. The results also show that the technique is sensitive enough to detect local Ca^{2+} depletions, elementary intra-SR signals associated with local Ca^{2+} signals, such as sparks.

Acknowledgments

The authors would like to thank Mrs. Marianne Courtehoux and Mr. Michael Kaenzig for expert technical assistance. This work was supported by a grant from the Swiss National Science Foundation (grant 31-156375) and the Microscopy Imaging Center (MIC) of the University of Bern.

References

- [1] J.P. Kao, A.T. Harootunian, R.Y. Tsien, Photochemically generated cytosolic calcium pulses and their detection by fluo-3, *J Biol Chem.* 264 (1989) 8179–8184.
- [2] A. Minta, J.P. Kao, R.Y. Tsien, Fluorescent indicators for cytosolic calcium based on rhodamine and fluorescein chromophores, *J Biol Chem.* 264 (1989) 8171–8178.
- [3] G. Grynkiewicz, M. Poenie, R.Y. Tsien, A new generation of Ca^{2+} indicators with greatly improved fluorescence properties, *J Biol Chem.* 260 (1985) 3440–3450.
- [4] G.A. Peeters, V. Hlady, J.H. Bridge, W.H. Barry, Simultaneous measurement of calcium transients and motion in cultured heart cells, *Am. J. Physiol.* 253 (1987) H1400–8.
- [5] J.D. Molkentin, J.R. Lu, C.L. Antos, B. Markham, J. Richardson, J. Robbins, et al., A calcineurin-dependent transcriptional pathway for cardiac hypertrophy, *Cell.* 93 (1998) 215–228.
- [6] D.M. Bers, D.A. Eisner, H.H. Valdivia, Sarcoplasmic reticulum Ca^{2+} and heart failure: roles of diastolic leak and Ca^{2+} transport, *Circ Res.* 93 (2003) 487–490.
- [7] M. Lindner, E. Erdmann, D.J. Beuckelmann, Calcium content of the sarcoplasmic reticulum in isolated ventricular myocytes from patients with terminal heart failure, *J Mol Cell Cardiol.* 30 (1998) 743–749.
- [8] I.A. Hobai, B. O'Rourke, Decreased sarcoplasmic reticulum calcium content is responsible for defective excitation-contraction coupling in canine heart failure, *Circulation.* 103 (2001) 1577–1584.
- [9] Z. Kubalova, D. Terentyev, S. Viatchenko-Karpinski, Y. Nishijima, I. Györke, R. Terentyeva, et al., Abnormal intrastore calcium signaling in chronic heart failure, *Proc Natl Acad Sci USA.* 102 (2005) 14104–14109.
- [10] N.A. Benkusky, E.F. Farrell, H.H. Valdivia, Ryanodine receptor channelopathies, *Biochem Bioph Res Comm.* 322 (2004) 1280–1285.
- [11] M.J. Betzenhauser, A.R. Marks, Ryanodine receptor channelopathies, *Pflugers Arch - Eur J Physiol.* 460 (2010) 467–480.
- [12] I. Györke, N. Hester, L.R. Jones, S. Györke, The role of calsequestrin, triadin, and junctin in conferring cardiac ryanodine receptor responsiveness to luminal calcium, *Biophys J.* 86 (2004) 2121–2128.
- [13] D. Jiang, Enhanced store overload-induced Ca^{2+} release and channel sensitivity to luminal Ca^{2+} activation are common defects of RyR2 mutations linked to ventricular tachycardia and sudden death, *Circ Res.* 97 (2005) 1173–1181.
- [14] W. Chen, R. Wang, B. Chen, X. Zhong, H. Kong, Y. Bai, et al., The ryanodine receptor store-sensing gate controls Ca^{2+} waves and Ca^{2+} -triggered arrhythmias, *Nat. Med.* 20 (2014) 184–192.
- [15] G. Callewaert, L. Cleemann, M. Morad, Caffeine-induced Ca^{2+} release activates Ca^{2+}

- extrusion via Na^+ - Ca^{2+} exchanger in cardiac myocytes, *Am. J. Physiol. Cell Physiol.* 257 (1989) C147–52.
- [16] A. Varro, N. Negretti, S.B. Hester, D.A. Eisner, An estimate of the calcium content of the sarcoplasmic reticulum in rat ventricular myocytes, *Pflugers Arch - Eur J Physiol.* 423 (1993) 158–160.
 - [17] N. Negretti, A. Varro, D.A. Eisner, Estimate of net calcium fluxes and sarcoplasmic reticulum calcium content during systole in rat ventricular myocytes, *J. Physiol. (Lond.)*. 486 (1995) 581–591.
 - [18] M.E. Díaz, A.W. Trafford, S.C. O'Neill, D.A. Eisner, Measurement of sarcoplasmic reticulum Ca^{2+} content and sarcolemmal Ca^{2+} fluxes in isolated rat ventricular myocytes during spontaneous Ca^{2+} release, *J. Physiol. (Lond.)*. 501 (1997) 3–16.
 - [19] A.V. Shmigol, D.A. Eisner, S. Wray, Simultaneous measurements of changes in sarcoplasmic reticulum and cytosolic $[\text{Ca}^{2+}]$ in rat uterine smooth muscle cells, *J. Physiol. (Lond.)*. (2001).
 - [20] C.A. Valverde, D. Kornyejev, M. Ferreira, A.D. Petrosky, A. Mattiazzi, A.L. Escobar, Transient Ca^{2+} depletion of the sarcoplasmic reticulum at the onset of reperfusion, *Cardiovasc Res.* 85 (2010) 671–680.
 - [21] D. Kornyejev, M. Reyes, A.L. Escobar, Luminal Ca^{2+} content regulates intracellular Ca^{2+} release in subepicardial myocytes of intact beating mouse hearts: effect of exogenous buffers, *Am J Physiol Heart Circ Physiol.* 298 (2010) H2138–H2153.
 - [22] A.A. Kabbara, D.G. Allen, The use of the indicator fluo-5N to measure sarcoplasmic reticulum calcium in single muscle fibres of the cane toad, *J. Physiol. (Lond.)*. 534 (2001) 87–97.
 - [23] T.R. Shannon, T. Guo, D.M. Bers, Ca^{2+} scraps: local depletions of free $[\text{Ca}^{2+}]$ in cardiac sarcoplasmic reticulum during contractions leave substantial Ca^{2+} reserve, *Circ Res.* 93 (2003) 40–45.
 - [24] D.X.P. Brochet, D. Yang, A. Di Maio, W.J. Lederer, C. Franzini-Armstrong, H. Cheng, Ca^{2+} blinks: rapid nanoscopic store calcium signaling, *Proc Natl Acad Sci USA.* 102 (2005) 3099–3104.
 - [25] T.L. Domeier, L.A. Blatter, A.V. Zima, Alteration of sarcoplasmic reticulum Ca^{2+} release termination by ryanodine receptor sensitization and in heart failure, *J. Physiol. (Lond.)*. 587 (2009) 5197–5209.
 - [26] D.X.P. Brochet, W. Xie, D. Yang, H. Cheng, W.J. Lederer, Quarky calcium release in the heart, *Circ Res.* 108 (2011) 210–218.
 - [27] J.M. Fawcett, S.M. Harrison, C.H. Orchard, A method for reversible permeabilization of isolated rat ventricular myocytes, *Experimental Physiology.* 83 (1998) 293–303.
 - [28] Y.-T. Zhao, C.R. Valdivia, G.B. Gurrola, P.P. Powers, B.C. Willis, R.L. Moss, et al., Arrhythmogenesis in a catecholaminergic polymorphic ventricular tachycardia mutation that depresses ryanodine receptor function, *Proc Natl Acad Sci USA.* 112 (2015) E1669–E1677.
 - [29] A.W. Trafford, G.C. Sibbring, M.E. Díaz, D.A. Eisner, The effects of low concentrations of caffeine on spontaneous Ca release in isolated rat ventricular myocytes, *Cell Calcium.* 28

(2000) 269–276.

- [30] A. Miyawaki, J. Llopis, R. Heim, J.M. McCaffery, J.A. Adams, M. Ikura, et al., Fluorescent indicators for Ca^{2+} based on green fluorescent proteins and calmodulin, *Nature*. 388 (1997) 882–887.
- [31] A.E. Palmer, C. Jin, J.C. Reed, R.Y. Tsien, Bcl-2-mediated alterations in endoplasmic reticulum Ca^{2+} analyzed with an improved genetically encoded fluorescent sensor, *Proc Natl Acad Sci USA*. 101 (2004) 17404–17409.
- [32] R. Rudolf, Direct in vivo monitoring of sarcoplasmic reticulum Ca^{2+} and cytosolic cAMP dynamics in mouse skeletal muscle, *J Cell Biol*. 173 (2006) 187–193.
- [33] P.P. Jones, D. Jiang, J. Bolstad, D.J. Hunt, L. Zhang, N. Demaurex, et al., Endoplasmic reticulum Ca^{2+} measurements reveal that the cardiac ryanodine receptor mutations linked to cardiac arrhythmia and sudden death alter the threshold for store-overload-induced Ca^{2+} release, *Biochem. J*. 412 (2008) 171.
- [34] L. Kaestner, A. Scholz, Q. Tian, S. Ruppenthal, W. Tabellion, K. Wiesen, et al., Genetically encoded Ca^{2+} indicators in cardiac myocytes, *Circ Res*. 114 (2014) 1623–1639.
- [35] H. Kasai, A. Yao, T. Oyama, H. Hasegawa, H. Akazawa, H. Toko, et al., Direct measurement of Ca^{2+} concentration in the SR of living cardiac myocytes, *Biochem Bioph Res Comm*. 314 (2004) 1014–1020.
- [36] E. Bovo, J.L. Martin, J. Tyryfter, P.P. deTombe, A.V. Zima, R-CEPIA1er as a new tool to directly measure sarcoplasmic reticulum [Ca] in ventricular myocytes, *Am J Physiol Heart Circ Physiol*. (2016) ajpheart.00175.2016–24.
- [37] P. Lipp, J. Hüser, L. Pott, E. Niggli, Spatially non-uniform Ca^{2+} signals induced by the reduction of transverse tubules in citrate-loaded guinea-pig ventricular myocytes in culture, *J. Physiol. (Lond.)*. 497 (1996) 589–597.
- [38] Y.N. Tallini, M. Ohkura, B.-R. Choi, G. Ji, K. Imoto, R. Doran, et al., Imaging cellular signals in the heart in vivo: Cardiac expression of the high-signal Ca^{2+} indicator GCaMP2, *Proc Natl Acad Sci USA*. 103 (2006) 4753–4758.

Figure captions:

Figure 1. Fluo-5N SR-loading and distribution in a mouse cardiomyocyte. A, 2D images show Fluo-5N and Rhod-2 distribution in a permeabilized mouse ventricular myocyte. The bright background fluorescence (Rhod-2 in the bath solution) has been subtracted, but some edge effects remain near the cell border. The triangle indicates a spontaneous Ca^{2+} wave which travelled across the cell during the slow confocal scanning process. Scale bar represents 20 μm . B, Pattern of Fluo-5N intensity measured along the longitudinal cell axis (yellow line in panel A). Fluorescence peaks correspond to junctional SR (JSR), valleys to free SR (FSR). C, 3D surface image of Fluo-5N and Rhod-2 in the cell shown in panel A). D, Distribution of Fluo-5N measured along a transversal line in the junctional and free SR region (see yellow line ROIs in panel C). E, Efficiency of Fluo-5N loading in presence of PMSF (100 $\mu\text{mol/L}$), BSA (0.5% w/v) or both. (Control: n=40, N=8; PMSF: n=25, N=3; BSA: n=54, N=10; PMSF+BSA: n=20, N=2).

Figure 2. Cytosolic Fluo-5N Ca^{2+} signal contamination in intact mouse cardiomyocytes. A, Image of Fluo-5N fluorescence distribution before (1) and during caffeine (10 mmol/L) application (3), to remove Ca^{2+} from the SR. Scale bar represents 20 μm . The cytosolic contamination also obscures the striation pattern of Fluo-5N loading. B, Scheme illustrates cytosolic Ca^{2+} signal due to contaminating Fluo-5N during large SR- Ca^{2+} release induced by caffeine. C, Representative traces of fluorescence signal in cells presenting Fluo-5N entrapped into the cytosol. D, Statistical analysis of fluorescence intensities in the different phases (1- before, 2- immediately after caffeine application and 3- plateaus during caffeine application) shown in panels A-C (N=4, n=6, *p=0.032).

Figure 3. Whole-cell patch clamp configuration to reduce cytosolic Fluo-5N contamination. A, Scheme illustrates how cell dialysis via a patch pipette can remove Fluo-5N entrapped into the cytosol, thereby reducing the contaminating cytosolic Fluo-5N signal. B, Representative line scan images and normalized fluorescence traces of cytosolic Ca^{2+} (Rhod-2 in red) and SR Ca^{2+} (Fluo-5N in green) during voltage-clamp depolarizations.

Figure 4. Irreversible permeabilization with saponin completely removes cytosolic Fluo-5N. A, Saponin binds to cholesterol in the plasma membrane generating pores. B, Caffeine application induces a maintained decrease in the SR Ca^{2+} signal (Fluo-5N) and a transient increase in the cytosolic Ca^{2+} concentration (Rhod-2). C, Representative line scan and trace of a spontaneous wave. The image was de-skewed to synchronize and analyse all pixel-lines with the same time-course during a Ca^{2+} wave. D, Representative line scan image and normalized traces of a localized cytosolic Ca^{2+} transient and its corresponding SR Ca^{2+} depletion.

Figure 5. Reversible permeabilization with SLO to reduce Fluo-5N contamination maintaining the electrical properties of the plasma membrane. A, SLO creates a temporal pore in the plasma membrane under reducing conditions. Contaminating Fluo-5N can diffuse out of the cell. B, Proof of concept showing retention of the membrane impermeable Rhod-2 after SLO-dependent permeabilization in Rhod-2 containing solution. To induce SR- Ca^{2+} overload and Ca^{2+} waves the cells were bathed with solution containing 6 mmol/L Ca^{2+} . Subsequently, 1 $\mu\text{mol/L}$ isoproterenol was added. C, Change of Ca^{2+} wave parameters confirming intact β -adrenergic signaling pathway after reversible permeabilization (N=2, n=3-6, * $p < 0.05$). D, De-skewed (for the second wave) SR Ca^{2+} waves recorded in 6 mmol/L extracellular Ca^{2+} . Note absence of fluorescence overshoot at beginning of waves, suggesting successful removal of residual Fluo-5N.

Figure 6. Experiments carried out to validate the technique. A, Application of a low concentration of caffeine (200 $\mu\text{mol/L}$) increases the luminal RyR Ca^{2+} sensitivity and gradually reduces the threshold to initiate Ca^{2+} waves. B, A high concentration of caffeine induces a decrease of SR Ca^{2+} signal to the minimal intensity, which can be used to normalize the Fluo-5N signals and correct for differences in Fluo-5N loading between cells.

Figure 1

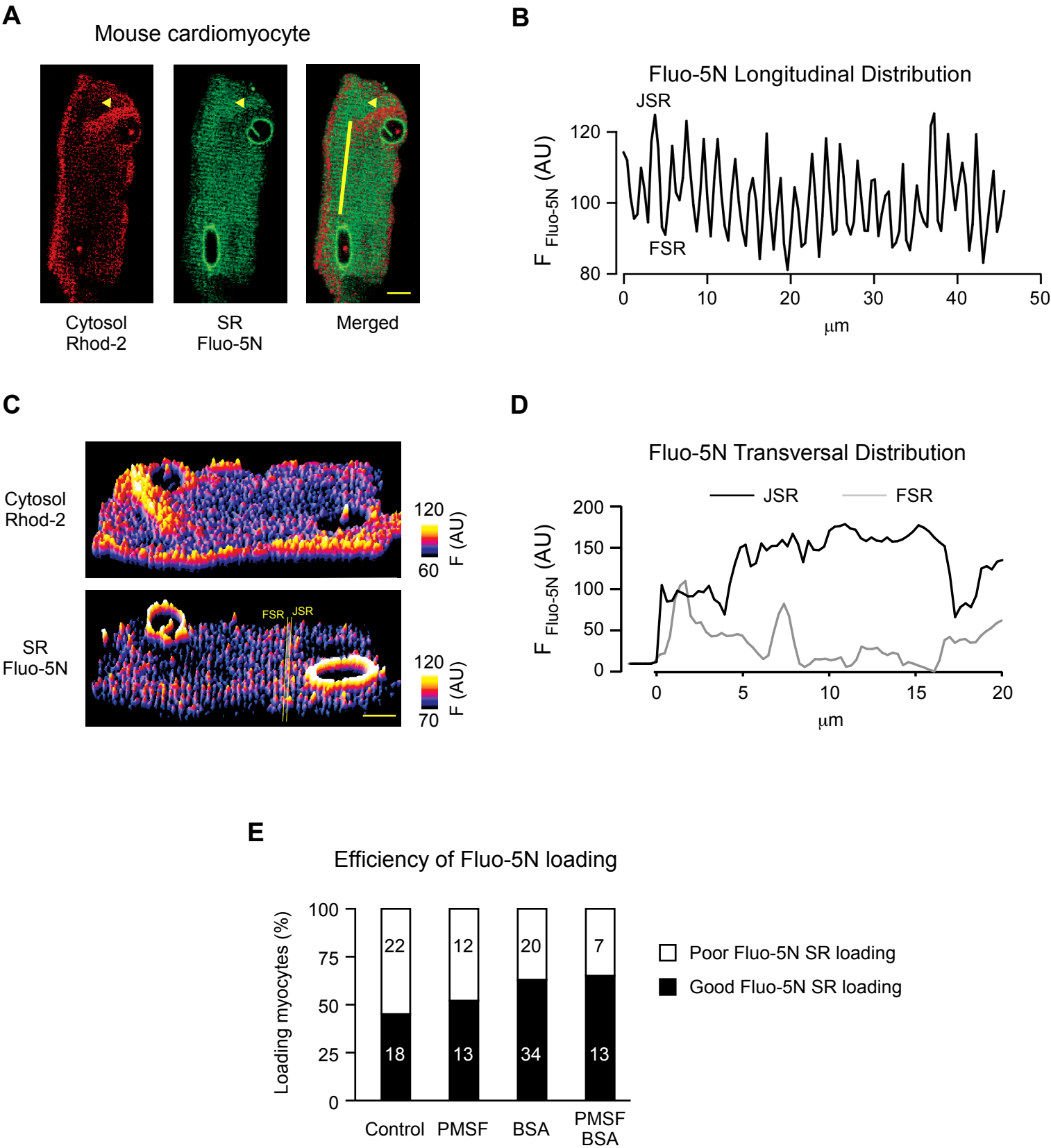
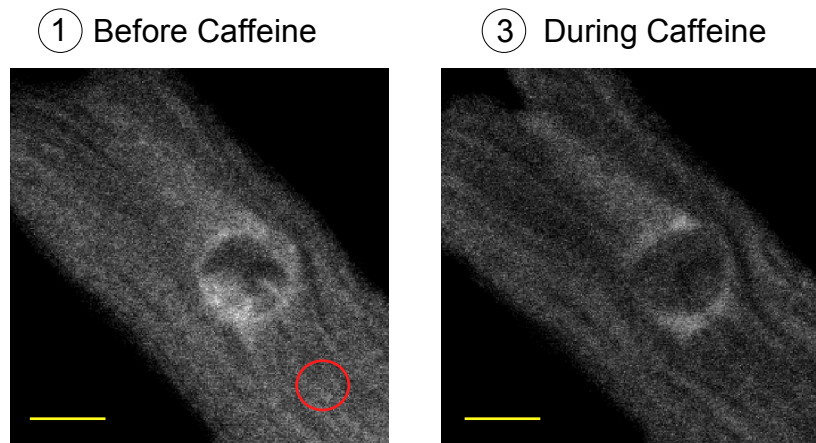
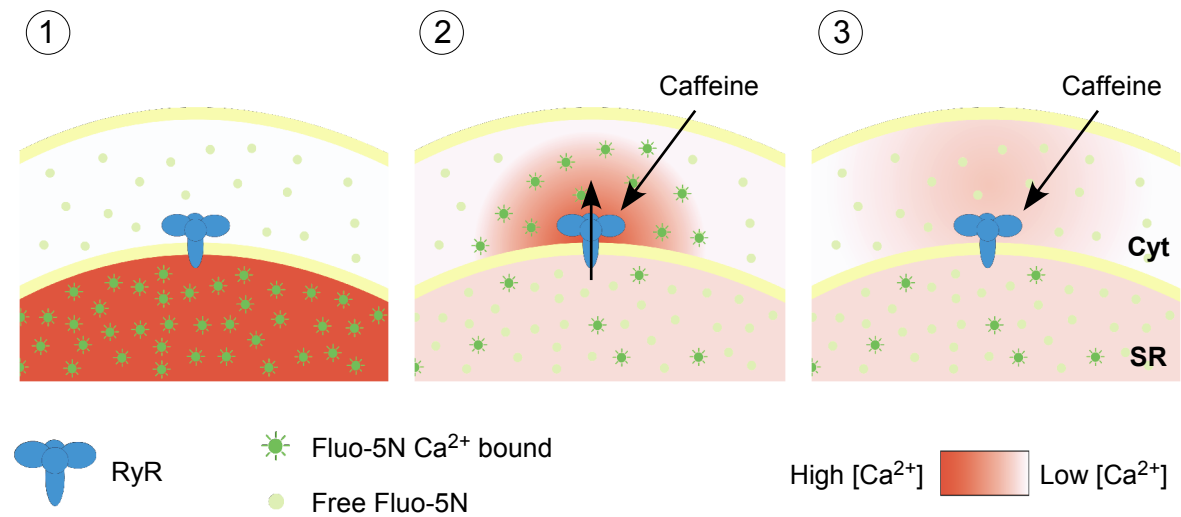


Figure 2

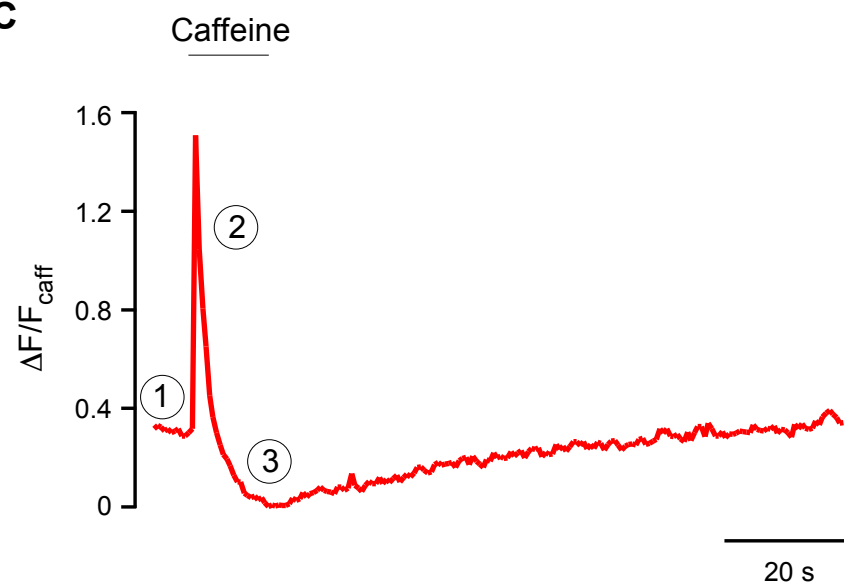
A



B



C



D

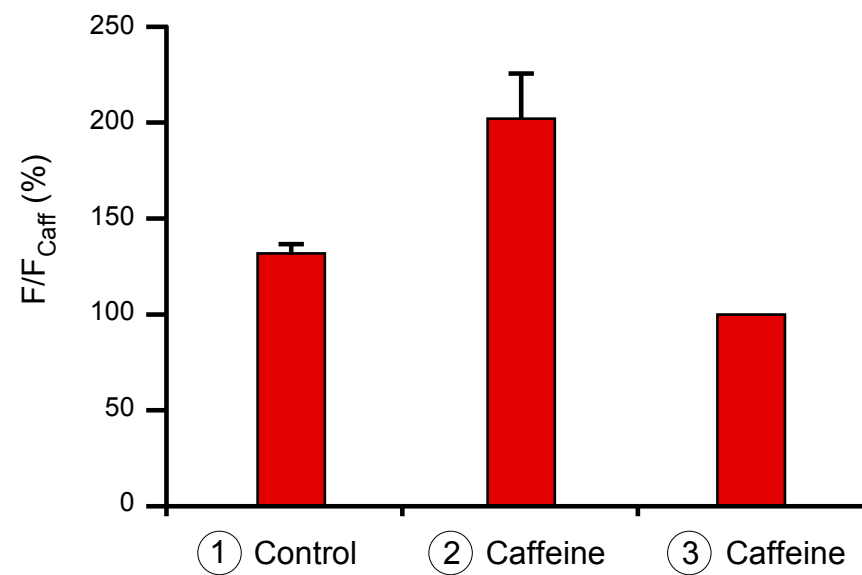


Figure 3

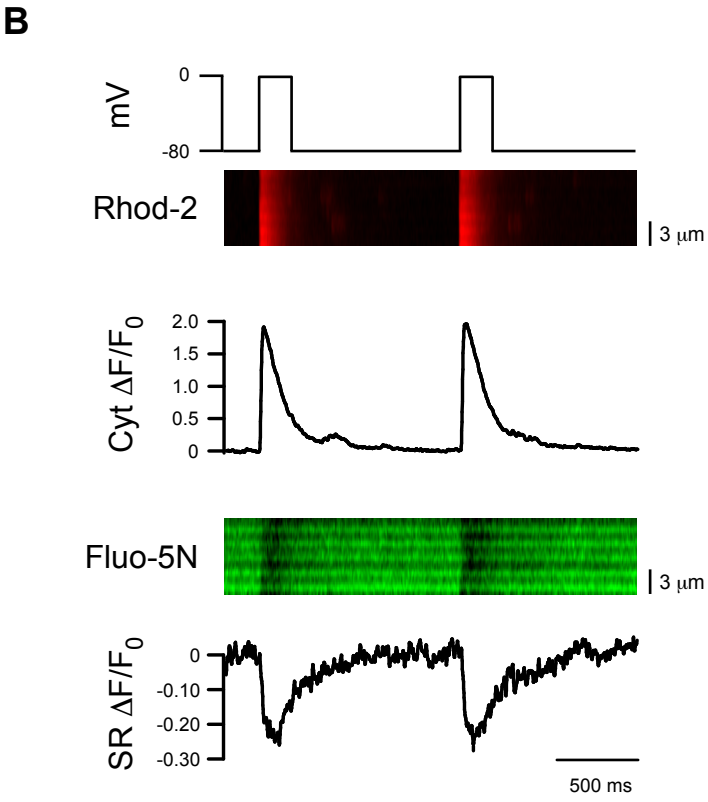
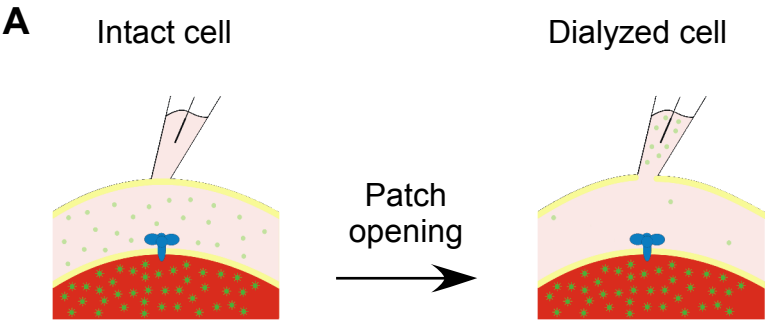
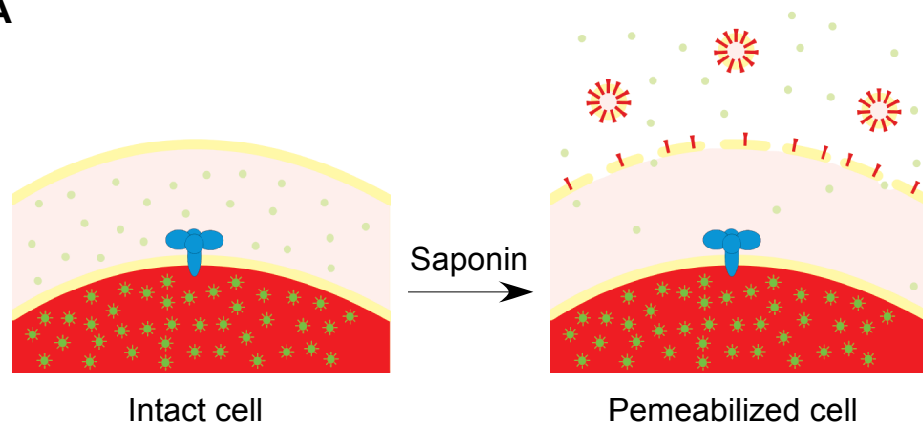
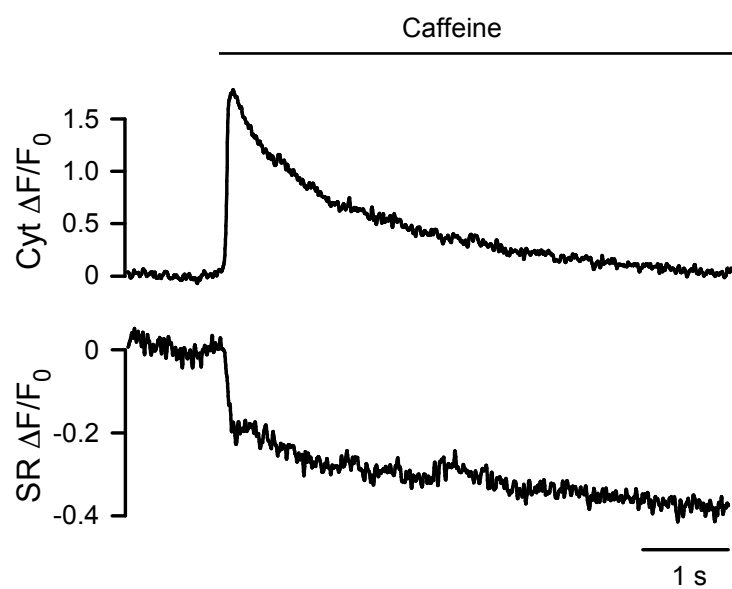
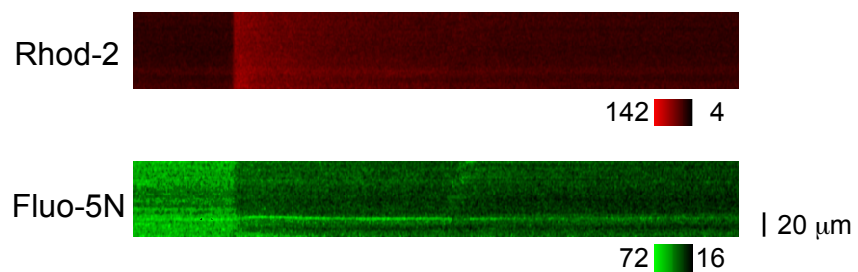


Figure 4

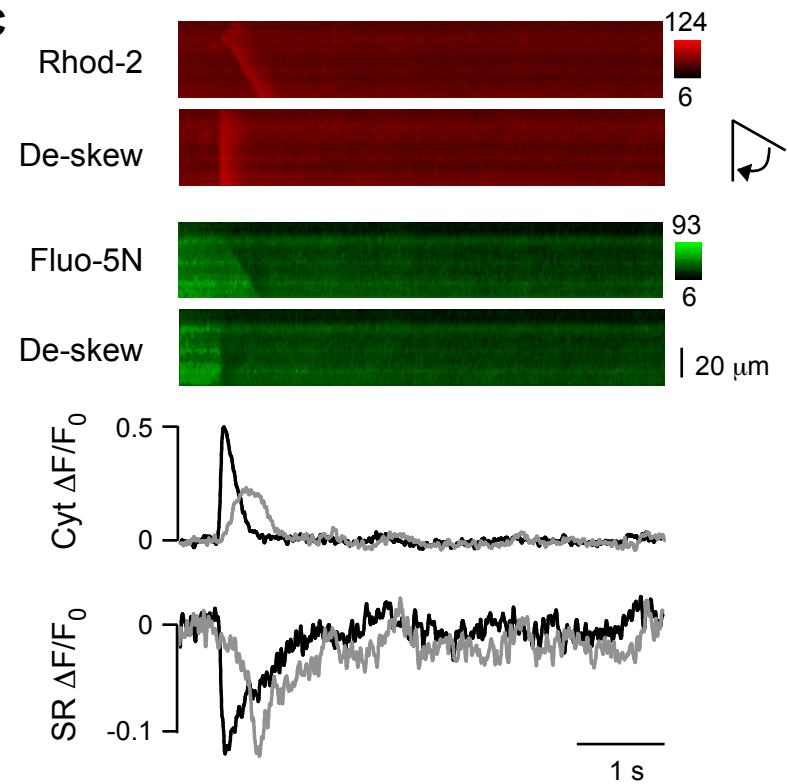
A



B



C



D

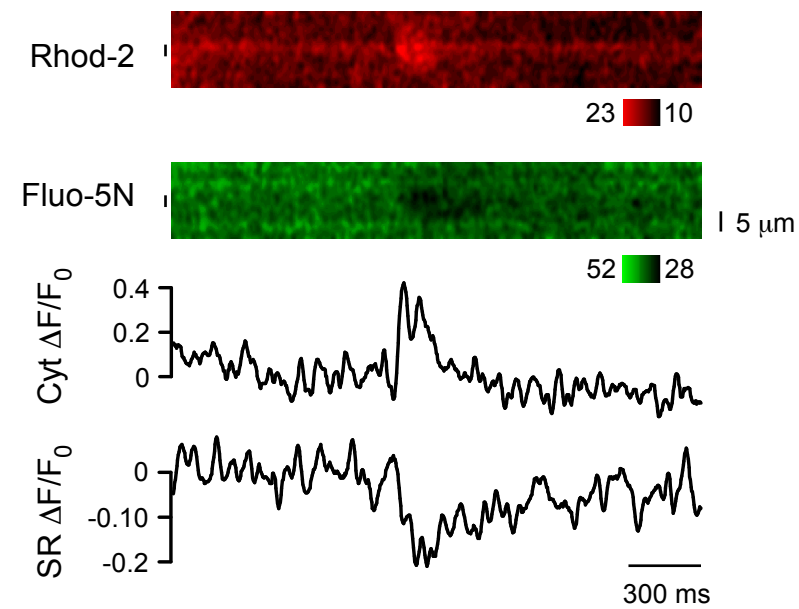


Figure 5

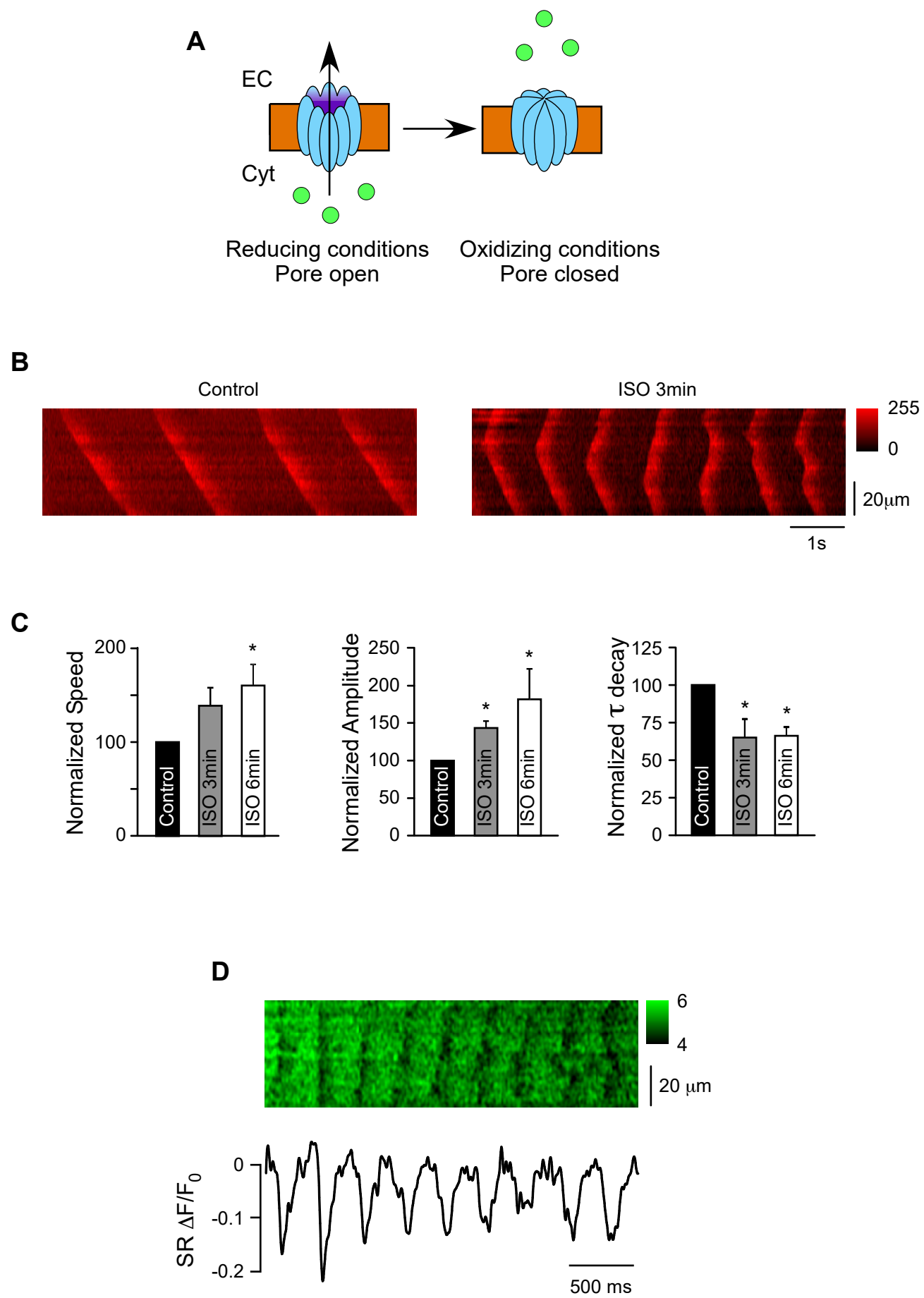
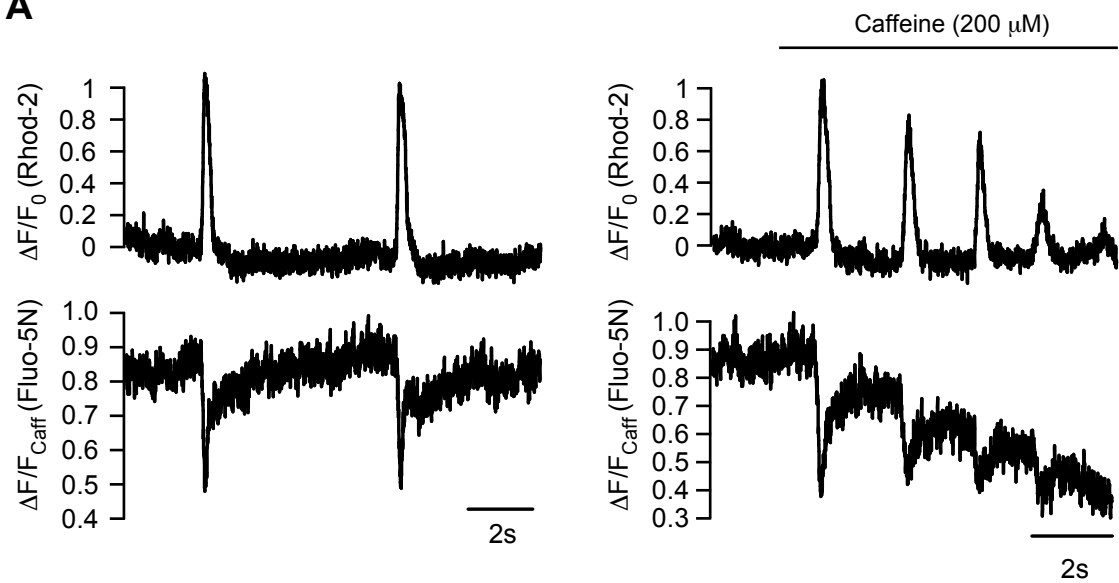


Figure 6

A



B

